Research Journal of Applied Sciences, Engineering and Technology 5(4): 1118-1122, 2013
DOI:10.19026/rjaset.5.4824
ISSN: 2040-7459; e-ISSN: 2040-7467

Submitted: May 06, 2012 Accepted: May 29, 2012 Published: February 01, 2013

**Research Article**

# Interpretation of the Phenomena of Heat Transfer from Representations of Nyquist and Bode Plots

K. Ould Cheikh, I. Diagne, M. L. Sow, M. S. Ould Brahim, A. Diouf, K. Diallo, M. Dieng and G. Sissoko
Laboratory of Semiconductors and Solar Energy, Physics Department, Faculty of Science and Technology, University Cheikh Anta Diop, Dakar, Senegal

**Abstract:** The thermal impedance of a tow-plaster material is determined from the thermal electrical analogy in the dynamic frequency regime. The thermophysical characteristics magnitudes of the material, thermal conductivity and coefficient of thermal diffusivity are relating to shunt and series resistances determined from the results of the study of representations of Nyquist and Bode plots. The study applied to the composite tow-plaster showed it can be used as a good thermal insulator.

**Keywords:** Impedance thermal, plaster, thermal insulator, tow

## INTRODUCTION

Thermal comfort (Meukam *et al*., 2004) in the building requires a good knowledge of heat transfer through the wall. Several materials (Bekkouche *et al*., 2007; Gaye *et al*., 2001) are used for making wall insulator to minimize energy loss or heating inside buildings. Achieving the thermal insulators walls requires a good characterization of materials by the determination of thermophysical properties (Voumbo *et al*., 2010; Jannot *et al*., 2009) materials. The thermal conductivity of the tow-plaster material is relating to serie resistance and to shunt resistance. These resistances are determined from the study of the thermal impedance. The Bode diagrams show the evolution of the thermal impedance in a frequency band of external climatic solicitations. Nyquist representations allow to obtain the thermal resistance of the material. The use of Bode diagrams and Nyquist representations (Dieng *et al*., 2007) allowed to propose an equivalent electrical model of the wall on the phenomena of storage and heat exchange.

## STUDY MODEL

The front wall is shown in Fig. 1. Table 1 and 2 are the respective temperatures of outdoor and indoor environments; h1y and h2y are the heat exchange coefficients corresponding. The heat exchange coefficients on the sides, h1x and h2x are supposed to very low, which allows to neglect the heat exchange at the sides.

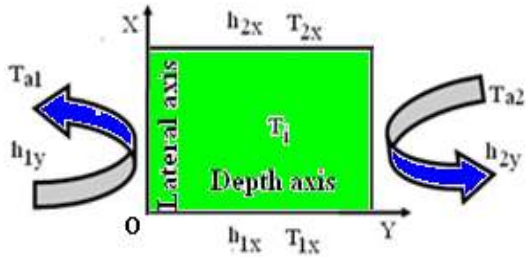


Fig. 1: Wall plane having regard in two dimensions
Ti: Initial temperature of the material assumed to be zero during the study; Ta1 and Ta2: the temperatures of indoor and outdoor environments; h1y and h2y: the convective heat transfer coefficients on the outer and inner faces; radiative coefficients are assumed negligible; h1x and h2x: the convective heat exchange coefficient on the lateral faces supposed low; T01: 25°C is the maximum ambient temperature to the outer face; T02: 10°C is the maximum ambient temperature to the inner face

The exploitation of the heat equation to two dimensions and in dynamic frequency regime, given the boundary conditions imposed on the wall (Ould Brahim *et al*., 2011), yields the expression (1) of the temperature. From this expression, we derive the expression (2) the density of heat flow:

$$T(x,y,t) = \sum_{n=1}^{\infty} (\cos(\beta_n \cdot x) + \frac{h_{1x}}{\lambda \cdot \beta_n} \cdot \sin(\beta_n \cdot x)) \quad (1)$$
$$(a_n \cdot \cosh(\mu_n \cdot y) + b_n \cdot \sinh(\mu_n \cdot y)) \cdot e^{i \cdot \omega \cdot t}$$

**Corresponding Author**: G. Sissoko, Faculty of Science and Technology, University Cheikh Anta Diop, Dakar, Senegal

Table 1: Eigenvalues $\beta_n$

| n | 1 | 2 | 3 | 4 | 5 | 6 | 7 | 8 | 9 | 10 | 11 | 12 |
|---|---|---|---|---|---|---|---|---|---|---|---|---|
| $\beta_n$ | 10.5 | 64.4 | 126.6 | 188.9 | 251.8 | 314.4 | 377.3 | 440 | 502.8 | 565.7 | 628.6 | 691.2 |

$a_n$ and $b_n$ the coefficients in Eq. (1) and (2) are given by the expressions (4) and (5)

Table 2: Series resistors and shunt of the wall plane

| | High heat exchange coefficient to the outer face | | High heat exchange coefficient at the inner- | |
|---|---|---|---|---|
| | $h1y = 5.10^{-3}$ W/m$^2$ h2y = 20 W/m$^2$ | $h1y = 5.10^{-4}$ W/m$^2$ h2y = 20 W/m$^2$ | h1y = 20 W/m$^2$ h2y = $5.10^{-3}$ W/m$^2$ | h1y = 20 W/m$^2$ h2y = $5.10^{-4}$ W/m$^2$ |
| Rs (°C/W) | -0.401 | -0.400 | 0.104 | 0.103 |
| Rsh (°C/W) | 0.208 | 0.202 | 0.451 | 0.454 |
| Rth = Rs+Rsh (°C/W) | 0.609 | 0.602 | 0.555 | 0.557 |

The uncertainty on the thermal resistance is a maximum of about $\Delta Rth/Rth = 9.5\%$

$$\varphi = \lambda \cdot \left[ \begin{array}{l} \mu_n{}^2 \cdot \left( \sum_{n=1}^{\infty} (\cos(\beta_n \cdot x) + \frac{h_{1x}}{\lambda \cdot \beta_n} \cdot \sin(\beta_n \cdot x)) \cdot (a_n \cdot sh(\mu_n \cdot y) + b_n \cdot ch(\mu_n \cdot y)) \right)^2 \\ + \beta_n{}^2 \cdot \left( \sum_{n=1}^{\infty} (-\sin(\beta_n \cdot x) + \frac{h_{1x}}{\lambda \cdot \beta_n} \cdot \cos(\beta_n \cdot x)) \cdot (a_n \cdot ch(\mu_n \cdot y) + b_n \cdot sh(\mu_n \cdot y)) \right)^2 \end{array} \right]^{\frac{1}{2}} \cdot e^{i \cdot \omega \cdot t} \quad (2)$$

with:

$$\mu_n = \sqrt{\beta_n{}^2 + \frac{i \cdot \omega}{\alpha}} = \sqrt{\beta_n{}^2 + \frac{\omega}{2 \cdot \alpha}(1+i)^2} \quad (3)$$

The eigenvalues $\beta_n$ (Table 1) are determined from transcendental equation (Ould Brahim *et al*., 2011) ;ω is the an gular frequency of the external climatic stresses; α is the coefficient of thermal diffusivity:

$$a_n = \frac{4 \cdot \lambda \cdot \beta_n \cdot \sin(\beta_n L) \left[ h_{1y} \cdot (\lambda \cdot \mu_n \cdot ch(\mu_n \cdot H) + h_{2y} \cdot sh(\mu_n \cdot H)) \cdot T_{01} + h_{2y} \cdot \lambda \cdot \mu_n \cdot T_{02} \right]}{D_n \left[ h_{1y} (\lambda \cdot \mu_n \cdot ch(\mu_n \cdot H) + h_{2y} \cdot sh(\mu_n \cdot H)) + \lambda \cdot \mu_n (\lambda \cdot \mu_n \cdot sh(\mu_n \cdot H) + h_{2y} \cdot ch(\mu_n \cdot H)) \right]} \quad (4)$$

$$b_n = \frac{h_{1y} \cdot 4 \cdot \lambda \cdot \beta_n \cdot \sin(\beta_n L) \cdot \left[ h_{2y} \cdot T_{02} - (\lambda \cdot \mu_n \cdot sh(\mu_n \cdot H) + h_{2y} \cdot ch(\mu_n \cdot H)) \cdot T_{01} \right]}{D_n \left[ h_{1y} (\lambda \cdot \mu_n \cdot ch(\mu_n \cdot H) + h_{2y} \cdot sh(\mu_n \cdot H)) + \lambda \cdot \mu_n (\lambda \cdot \mu_n \cdot sh(\mu_n \cdot H) + h_{2y} \cdot ch(\mu_n \cdot H)) \right]} \quad (5)$$

$$D_n = \left[ \lambda \cdot \beta_n \cdot (\sin(2\beta_n L) + 2\beta_n L) + h_{1x} \cdot (1 - \cos(2\beta_n L)) \right] \quad (6)$$

From the expressions of the temperature and density of heat flow through the material, we obtain the Eq. (7) giving the thermal impedance of the material under dynamic frequency regime:

$$z_e = \frac{\Delta T}{\varphi} = \frac{\sum_{n=1}^{\infty} a_n - (\cos(\beta_n \cdot x) + \frac{h_{1x}}{\lambda \cdot \beta_n} \cdot \sin(\beta_n \cdot x)) \cdot (a_n \cdot \cosh(\mu_n \cdot y) + b_n \cdot \sinh(\mu_n \cdot y))}{\lambda \cdot \left[ \begin{array}{l} \mu_n{}^2 \cdot \left( \sum_{n=1}^{\infty} (\cos(\beta_n \cdot x) + \frac{h_{1x}}{\lambda \cdot \beta_n} \cdot \sin(\beta_n \cdot x)) \cdot (a_n \cdot sh(\mu_n \cdot y) + b_n \cdot ch(\mu_n \cdot y)) \right)^2 \\ + \beta_n{}^2 \cdot \left( \sum_{n=1}^{\infty} (-\sin(\beta_n \cdot x) + \frac{h_{1x}}{\lambda \cdot \beta_n} \cdot \cos(\beta_n \cdot x)) \cdot (a_n \cdot ch(\mu_n \cdot y) + b_n \cdot sh(\mu_n \cdot y)) \right)^2 \end{array} \right]^{\frac{1}{2}}} \quad (7)$$

Of this Eq. (7) of the thermal impedance of the material, we study the Bode diagram and the Nyquist representations.

## RESULTS

**Bode diagram:** Figure 2 and 3 show, respectively the evolution of the thermal impedance and its phase according to the pulse exciting the temperature of the surrounding environment of the wall plane. In each figure we observe the behavior of the thermal impedance and its corresponding phase assuming that the heat transfer coefficient is high at the side in contact with the external medium (Fig. 2a and 3a) or the coefficient of heat exchange is relatively low at the side in contact with the internal environment to isolated (Fig. 2b and 3b).

Figure 2 and 3 are obtained for a position y = 2.5.10-2 m, in the middle of the wall plane between the faces in contact with the external environment and internal environment. For a heat exchange coefficient relatively large in outer face and small in the inner face (Fig. 2a and 3a), the module of the thermal impedance is order 0.1 °C/W and the phase of the impedance evolves of the null value corresponding to resonance phenomena to a maximum value of about $0.78 \approx \pi/4$ rad, before stabilizing around 0.4 rad

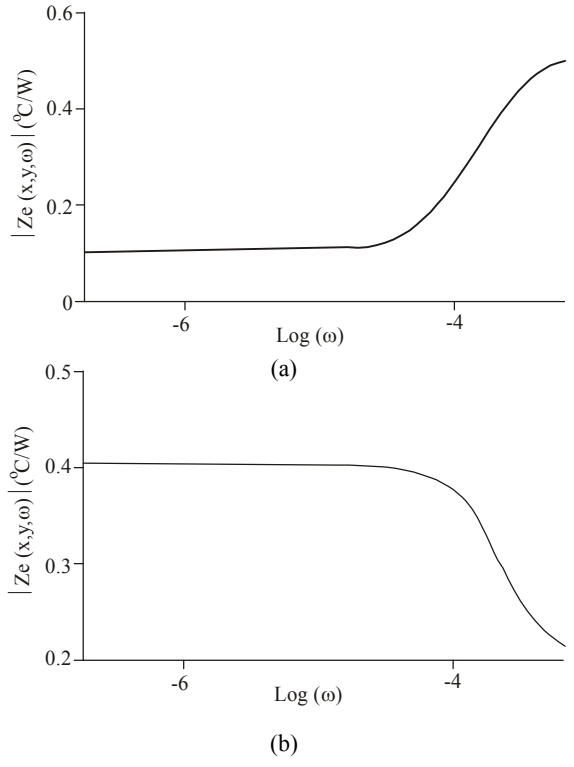


Fig. 2: Evolution of the thermal impedance as a function of the exciter pulse
λ: 0.063 W/m/°C; α: 8,285.10$^{-7}$ m$^2$/s; x: 0.025 m ; y: 0.025 m; a) h1y: 20 W/m$^2$/°C; h2y: 0.005 W/m$^2$/°C; b) h1y: 0.005 W/m$^2$/°C; h2y: 20 W/m$^2$

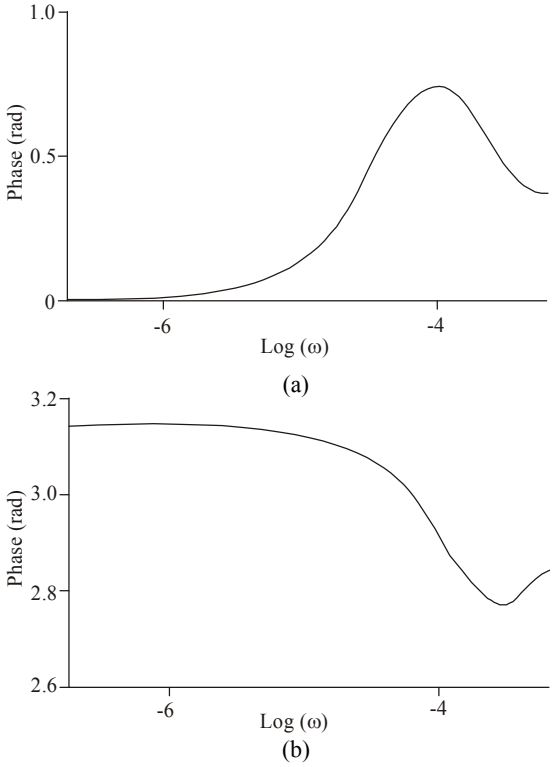


Fig. 3**:** Evolution of the phase of the impedance as a function of the excitation frequency
λ: 0.063 W/m/°C; α: 8,285.10$^{-7}$ m$^2$/s; x: 0.025 m ; y: 0.025 m; a) h1y: 20 W/m$^2$/°C; h2y: 0.005 W/m$^2$/°C; b) h1y: 0.005 W/m$^2$/°C; h2y: 20 W/m$^2$/°C

For against, for a heat exchange coefficient relatively low to the outside face (screening effect with respect to the outdoor heat) and important to the inner face (Fig. 2b and 3b), the modulus of the thermal impedance is of the order of 0.4 °C/W ; the phase of the impedance evolving to the value 3.14 rad corresponding to phenomena of antiphase between the inductive and capacitive equivalent circuit model, at a minimum value of about 2.75 rad, before stabilizing around 2.82 rad.

Cover the exterior wall of a unfavorable layer to the heat exchanges (smooth reflector), thus increases the thermal impedance of the material which improves the thermal comfort inside the building.

**Nyquist representation:** Figure 4 shows the evolution of the imaginary part of the thermal impedance as a function of its real part. Figure 4a shows the case where the heat exchange coefficient is high in outer face and to the Fig. 4b corresponds to the case where the heat exchange coefficient is elevated to the inner face, the outer face thus behaving like a screen of heat.

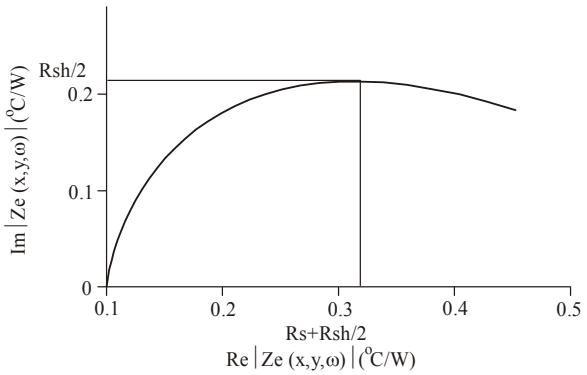


(a)

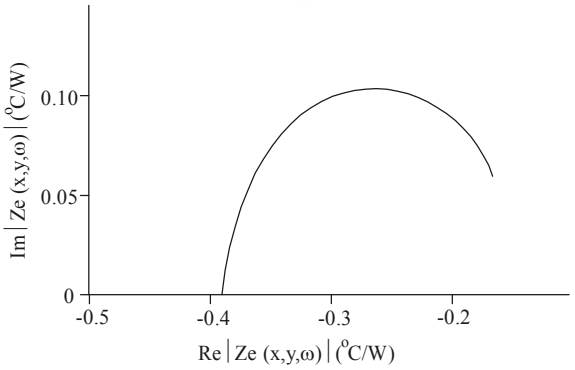


(b)

Fig. 4: Evolution of the imaginary part depending on the real part of the thermal impedance
λ: 0.063 W/m/°C; α: 8,285.10-7 m2/s; x: 0.025 m ; y: 0.025 m; a) h1y: 20 W/m2/°C; h2y: 0.005 W/m2/°C; b) h1y: 0.005 W/m2/°C; h2y: 20 W/m2/°C

Table 2 summarizes the different results obtained during this study. The comparison with the results of Bode shows that for low pulse excitation, the modulus of the thermal impedance is equal to the absolute value of the series Resistor (Rs). The negative resistance series reflects the effect shielding of heat for a low coefficient of heat exchange to the outside.

The shunt resistance (Rsh) of the material reflects heat loss compared to inductive and capacitive phenomena.

The thermal résistance (Rth) defined as a sum of the series resistor and shunt resistor is practically constant, Rth ≈ 0.60 °C/W. The overall thermal resistance reflects the phenomena of heat transfer by conduction.

**Equivalent circuit model:** The Fig. 5 is a proposed equivalent circuit model for studying the wall in dynamic frequency regime. RS1 and RS2 are respectively the series resistance of the flat wall to the

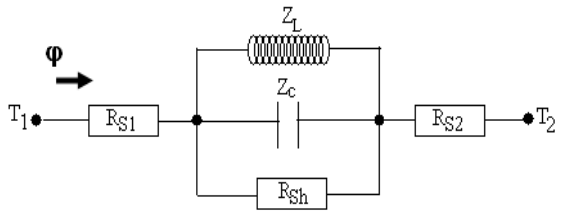


Fig. 5: Equivalent circuit diagram

outer face and to inner face; ZL and Zc correspond respectively to the impedance of the coil and the equivalent capacitance of stortage of heat; Rsh is shunt resistance. The total series resistance of the wall plane is Rs = Rs1+Rs2.

Expression of the thermal impedance equivalent material:

$$Ze = R_s + \frac{Z_L \cdot Z_C \cdot R_{Sh}}{Z_L \cdot R_{Sh} + Z_C \cdot R_{Sh} + Z_L \cdot Z_C} \quad (8)$$

With:

$$Z_L = jL\omega \quad (9)$$

$$Z_C = -\frac{j}{c\omega} \quad (10)$$

We define the inherent frequency of the material:

$$\omega_0 = \frac{1}{\sqrt{L \cdot c}}$$

Expression of the real part of the impedance:

$$R_e(Z_e) = R_s + \frac{L^2 \cdot \frac{R_{Sh}}{c^2}}{\frac{L^2}{c^2} + R_{Sh}^2 (L\omega - \frac{1}{c\omega})^2} \quad (11)$$

$$I_m(Z_e) = \frac{-R_{Sh}^2 \cdot \frac{L}{c} (L\omega - \frac{1}{c\omega})}{\frac{L^2}{c^2} + R_{Sh}^2 (L\omega - \frac{1}{c\omega})^2} \quad (12)$$

The limit values of the real part and imaginary part of the thermal impedance are given by Eq. (13), (14) and (15). Relations (16) and (17) are consistent with the method of determination of Rs and Rsh from Nyquist représentations (Fig. 4):

$$\lim_{\omega \to \omega_0} \mathrm{Re}(Z_e) = R_S + R_{Sh} \quad (13)$$

$$\lim_{\omega \to 0} \mathrm{Re}(Z_e) = R_S \quad (14)$$

$$\lim_{\omega \to 0} I_m(Z_e) = 0 \quad (15)$$

$$I_m(Z_e) = \frac{R_{Sh}}{2} \quad (16)$$

$$R_e(Z_e) = R_S + \frac{R_{Sh}}{2} \quad (17)$$

The cutoff frequency ωc = f (L, c, RSh) is given by the Eq. (18) and is determined from the expression (16) corresponding to the maximum of the curves in Fig. 4:

$$\omega_c = \frac{1}{2R_{Sh} \cdot c} + \frac{1}{2}\sqrt{\frac{1}{R_{sh}^{\ 2} \cdot c^2} + \frac{4}{L \cdot c}} \quad (18)$$

## CONCLUSION

The study shows the importance of thermal insulation in the thermal comfort of buildings. The material behavior tow-plaster the face of external climatic stresses shows that for thermal comfort, it is important to cover the outside walls with a insulator treated to reduce the heat transfer coefficient on this surface.

## ACKNOWLEDGMENT

Many thanks to all those whose work is cited to illustrate this study. We also thank the research team of Professor Gregory Sissoko at the University of Dakar, Senegal.

## RÉFÉRENCES

Bekkouche, S.M.A., T. Benouaz and A. Cheknane, 2007. Simulation study of the effect of thermal insulation of a piece of habitat in the region of Ghardaia. Revue des Energies Renouvelables, 10(2): 281-292.

Dieng, A., L. Ould Habiboulahy, A.S. Maïga, A. Diao and G. Sissoko, 2007. Impedance spectroscopy method applied to electrical parameters determination on bifacial silicon solar cell under magnetic field. J. Des Sci., 7(3): 48-52.

Gaye, S., F. Niang, I.K. Cissé, M. Adj, G. Menguy and G. Sissoko, 2001. Characterisation of thermal and mechanical properties of polymer concrete recycled. J. Sci., 1(1): 53-66.

Jannot, Y., A. Degiovanni and G. Payet, 2009. Thermal conductivity measurement of insulating materials with a three layers device. Int. J. Heat Mass Tran., 52: 1105-1111.

Meukam, P., Y. Jannot, A. Noumow and T.C. Kofan, 2004. Thermo physical characteristics of economical building materials. Constr. Build. Mater., 18: 437-443.

Ould Brahim, M.S., I. Diagne, S. Tamba, F. Niang and G. Sissoko, 2011. Characterization of the minimum effective layer of thermal insulation material tow-plaster from the method of thermal impedance. Res. J. Appl. Sci. Eng. Technol., 3(4): 337-343.

Voumbo, M. L., A. Wareme and G. Sissoko, 2010. Characterization of local Insulators: Sawdust and wool of kapok. Res. J. Appl. Sci. Eng. Technol., 2(2): 138-142.